Journal of Neuro-Oncology
https://doi.org/10.1007/s11060-024-04910-0

RESEARCH

MR perfusion characteristics of pseudoprogression in brain tumors treated with immunotherapy – a comparative study with chemo-radiation induced pseudoprogression and radiation necrosis

Hongyan Chen[1] · Guirong Tan[2,3] · Lijuan Zhong[4] · Yichuan Hu[3] · Wenjing Han[5] · Yi Huang[6] · Qiong Liang[7] · Denes Szekeres[8] · Haihui Jiang[9] · Rajnish Bharadwaj[10] · Stephen M. Smith[11] · Henry Z. Wang[11] · Xiang Liu[2,3]

Received: 21 October 2024 / Accepted: 6 December 2024

Abstract

Purpose Pseudoprogression is an atypical imaging pattern of response to immunotherapy in patients with brain tumors. MR perfusion studies in this field are limited. The purpose of our study is to compare the perfusion features between pseudoprogression lesions in malignant gliomas and brain metastases treated with immunotherapy (iPsP) and the pseudoprogression after chemo-radiation therapy and radiation necrosis after radiation treatment (ChR-PsP & RN).

Methods We retrospectively reviewed 25 iPsP lesions in 16 brain tumor patients and 48 ChR-PsP & RN lesions in 35 patients. The cerebral blood volume (CBV) of MR dynamic susceptibility contrast (DSC) perfusion weighted imaging (PWI) was analyzed, and the mean and maximal values of the ratio of CBV ($rCBV_{mean}$ and $rCBV_{max}$) of iPsPs and ChR-PsP & RNs were calculated and compared between these two groups using the Mann-Whitney U test. A receiver operating characteristic curve analysis was conducted, and the optimal cutoff of perfusion parameters were determined using the area under the curve, sensitivity, and specificity.

Results The medians of $rCBV_{mean}$ and $rCBV_{max}$ in iPsP group were significantly higher (0.94 and 1.39 respectively) than ChR-PsP & RN group (0.67, $p < 0.01$ and 1.1, $p = 0.01$ respectively). The $rCBV_{mean}$ value of 0.69 can differentiate the iPsP from ChR-PsP & RN with the area under the curve of 0.71, sensitivity of 0.72, and specificity of 0.56.

Conclusion These findings may suggest immunotherapy-induced higher perfusion in the iPsP lesions compared to ChR-PsP & RN lesions in primary and metastatic brain tumors.

Keywords Brain tumor · Tumor progression · Pseudoprogression · Immunotherapy · MR perfusion imaging

Hongyan Chen and Guirong Tan contributed equally to this work and share first authorship.

✉ Henry Z. Wang
Henry_Wang@URMC.Rochester.edu

✉ Xiang Liu
liuxiangxl72@163.com

[1] Department of Radiology, Beijing Tiantan Hospital, Capital Medical University, Beijing, China

[2] Advanced Neuroimaging Laboratory, The Affiliated Yuebei People's Hospital of Shantou University Medical College, Shaoguan, Guangdong Province, China

[3] Department of Radiology, The Affiliated Yuebei People's Hospital of Shantou University Medical College, Shaoguan, Guangdong Province, China

[4] Department of Pathology, The Affiliated Yuebei People's Hospital of Shantou University Medical College, Shaoguan, Guangdong Province, China

[5] Yanjing Medical College, Capital Medical University, Beijing, China

[6] Interventional Radiotherapy Room, The Affiliated Yuebei People's Hospital of Shantou University Medical College, Shaoguan, Guangdong Province, China

[7] Department of Pathology, The Third Affiliated Hospital of Sun Yat-Sen University, Guangzhou, China

[8] University of Rochester School of Medicine and Dentistry, Rochester, NY, USA

[9] Department of Neurosurgery, Peking University Third Hospital, Peking University, Beijing, China

[10] Department of Pathology and Laboratory Medicine (SMD), University of Rochester Medical Center, Rochester, NY, USA

[11] Department of Imaging Sciences, University of Rochester Medical Center, Rochester, NY, USA

Published online: 17 December 2024

Abbreviations

iPsP	Immunotherapy induced pseudoprogression
TP	Tumor progression
GBM	Glioblastoma
PWI	Perfusion-weighted imaging
ChR-PsP & RN	The pseudoprogression after chemo-radiation therapy and radiation necrosis after radiation treatment
ICI	Immune checkpoint inhibitor
BM	Brain metastases
DSC	Dynamic susceptibility contrast
CBV	Cerebral blood volume
RN	Radiation necrosis
ROC	Receiver operating characteristic
AUC	Area under curve
ChR-PsP & RN-BM	BM patients with ChR-PsP & RN (ChR-PsP & RN-BM)
T2WI	T2-weighted
DWI	Diffusion-weighted imaging
ADC	Apparent diffusion coefficient
T1-BRAVO	T1-weighted brain volume imaging with optimized gradient echo
T1-FLAIR	T1-weighted fluid-attenuated inversion recovery
ATRX	Alpha-thalassemia/mental retardation syndrome X-linked
DCE	Dynamic contrast-enhanced
ASL	Arterial spin labeling
CBF	Cerebral blood flow

Introduction

The pseudoprogression is defined as a phenomenon of the appearance of new lesion(s) or an increase in contrast-enhancing areas, but these changes gradually fade or stabilize without changing the treatment [1–5]. And the pseudoprogression refers to treatment-related clinic-radiologic changes instead of tumor progression (TP). The incidence of pseudoprogression is high (up to 30-40%) in the first 12 weeks after chemoradio-therapy for glioblastomas (GBM) [1], and it is difficult to differentiate between pseudoprogression and TP given the similarity of conventional MRI [1–5]. MR perfusion-weighted imaging (PWI), is an advanced MRI technique to evaluate hemodynamic status in brain tumors. Neoangiogenesis in malignant brain tumors results in elevated perfusion in TP. In contrast, the necrotic tissue and treatment-related damage in the pseudoprogression after chemoradio-therapy and radiation necrosis after radiation treatment (ChR-PsP & RN), leads to the decreased perfusion in these regions of malignant brain tumors. Thus, MR PWI has been used as an important tool to distinguish ChR-PsP & RN from TP [6–14].

In the past decades, immunotherapy including immune checkpoint inhibitors (ICIs), cancer vaccines, oncolytic viruses, adoptive cell therapy, and cytokines, has revolutionized the treatment of multiple aggressive solid tumors [15–17]. Recently, immunotherapy has emerged as a potential treatment option for primary and metastatic brain tumors with varying degrees of success [18]. Subsequently, immunotherapy induced pseudoprogression (iPsP), the atypical imaging pattern of response to immunotherapy, has been increasingly recognized in patients with malignant gliomas and brain metastases (BM) treated with immunotherapy. MR PWI studies of iPsP in brain tumors are limited. The purpose of this study is to evaluate the perfusion features of iPsPs in brain tumors, with a focus on the comparison to the ChR-PsP & RN.

Methods and materials

This retrospective study was approved by the ethics committees of our hospital, and the requirement for informed consent was waived. We reviewed MRI of 861 cases in both institutions with malignant gliomas and BM who received immunotherapy or chemo-radiation treatment or radiation therapy, from January 2015 to October 2023.

Patient selection

Based on the RANO criteria, the enrollment criteria of pseudoprogression and radiation necrosis included [1, 5, 19]: (1) the initial post-treatment MR examinations were performed within the first 6 months after the completion of immunotherapy, chemo-radiation therapy, or radiation therapy; (2) transient enlargement of primary lesion(s) size or the appearance of new lesion(s); (3) these lesions decrease in size or stabilize without additional treatments in the follow-up examinations, or histopathology diagnosis of resected lesions.

Patients were included in the study based on the following MRI enrollment criteria: (1) MR dynamic susceptibility contrast (DSC) PWI examination was acquired at the time of increasing lesion size; (2) pseudoprogression and radiation necrosis were diagnosed by surgical/histopathology diagnosis or follow-up MRI examinations which were performed with time interval $\geqq$ 4 weeks and follow-up MR examinations confirmed stabilization or decrease of lesion size. Patients with unsatisfactory preoperative images, or incomplete MRI examination were excluded. The workflow chart was seen in Fig. 1.

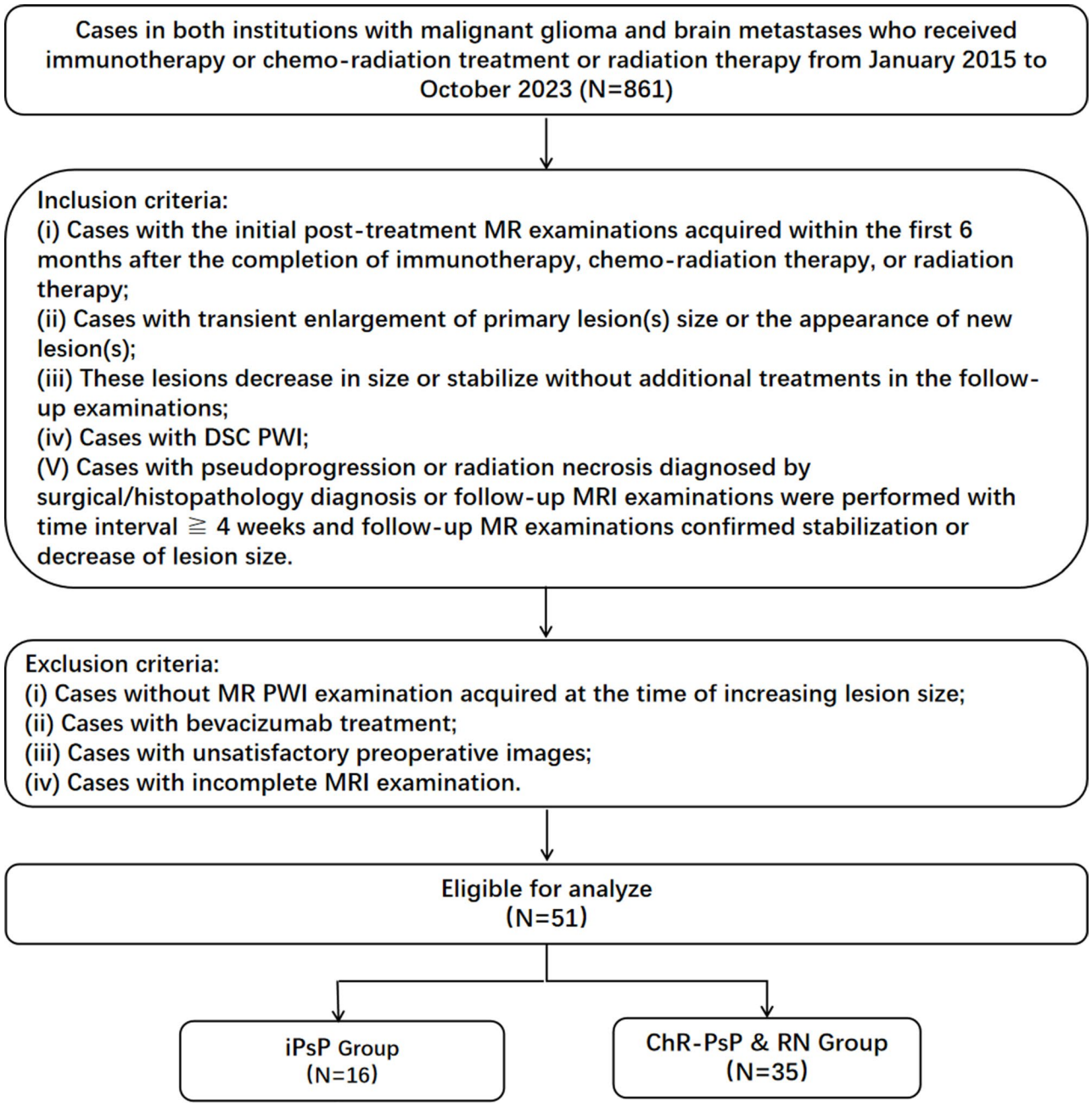

Fig. 1 The workflow chart of patient enrollment

The tumor size was assessed using two-dimensional tumor measurement based on RANO 2.0 criteria [1].

MR DSC-PWI scan and post-processing analysis

The MRI examinations were acquired using five MRI scanners (GE Signa HDxt, GE Discovery MR750w, GE Discovery MR750, Siemens Symphony, and Siemens MAG-NETOM Vida).

DSC-PWI was then performed with single-shot gradient-recalled echo-planar imaging (GRE-EPI) sequence (TR/TE = 1,525 ms/minimum, 250 Hz/pixel bandwidth, FOV = 24 × 24 cm, 1.0 × 1.0 × 5 mm voxel size, flip angle = 90°, matrix = 128 × 128, slice thickness = 5 mm, slice gap = 1 mm, NEX = 1). Fifty images were obtained for each slice. After ten phases, 0.1 mmol/kg Gd-DTPA (Bayer Schering Pharma AG, Berlin, Germany) was injected at a rate of 5 ml/sec, immediately followed by a 20 ml bolus of saline at the same injection rate.

Functool software (AW 4.6, GE Healthcare, Milwaukee, WI, USA) was used for the post-processing analysis of MR DSC-PWI. After the generation of the cerebral blood

Table 1 rCBV values of iPsP and ChR-PsP & RN

Group	iPsP ($n=16$)	ChR-PsP & RN			P_1	P_2	P_3	P_4
		Total ($n=35$)	BM($n=18$)	Glioma ($n=17$)				
Age(mean ± SD)	60.63 ± 10.84	58.43 ± 11.63	62.83 ± 8.42	53.76 ± 12.92	0.53	0.51	0.11	0.02
Size(median [IQR])	1.43 [0.89, 3.46]	2.64 [1.14, 6.60]	2.11 [1.14, 5.94]	3.23 [1.19, 7.18]	0.045	0.08	0.08	0.76
$rCBV_{mean}$(median [IQR])	0.94 [0.65, 1.61]	0.67 [0.35, 0.97]	0.73 [0.52, 0.95]	0.48 [0.28, 0.99]	< 0.01	0.03	< 0.01	0.25
$rCBV_{max}$(median [IQR])	1.39 [0.97, 3.25]	1.11 [0.53, 1.54]	1.05 [0.52, 1.30]	1.11 [0.51, 2.02]	0.01	0.01	0.08	0.54

iPsP: Immunotherapy induced pseudoprogression; ChR-PsP & RN: Pseudoprogression after chemoradio-therapy and radiation necrosis after radiation treatment. P_1: p-value for the difference in parameters between iPsP and ChR-PsP & RN. P_2: p-value for the difference in parameters between iPsP and ChR-PsP & RN-BM. P_3: p-value for the difference in parameters between iPsP and ChR-PsP & RN-Glioma. P_4: p-value for the difference in parameters between ChR-PsP & RN-BM and ChR-PsP & RN-Glioma

volume (CBV) map, semi-quantitative perfusion evaluation was obtained as the following process. First, four to six regions of interest (ROIs), each ranging from 38 to 45 mm^2 in size, were placed in the enhancing tumor to record the CBV value. An additional ROI was placed in the contralateral normal-appearing white matter as a reference. Two neuroradiologists, each with over 20 years of experience, conducted the placements of ROIs. The mean and maximal ratios of CBV ($rCBV_{mean}$ and $rCBV_{max}$) were calculated using mean and maximal CBV values of enhancing tumor divided by CBV values of reference white matter, respectively.

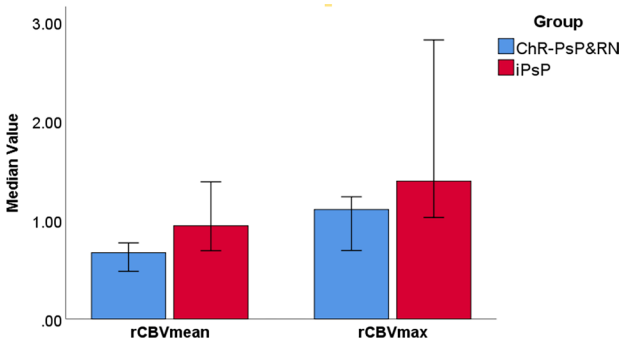

Fig. 2 Box-plots of median values of $rCBV_{mean}$ and $rCBV_{max}$ in iPsP and ChR-PsP & RN groups. The median values of $rCBV_{mean}$ and $rCBV_{max}$ in the group of iPsP were significantly higher than the median values of $rCBV_{mean}$ and $rCBV_{max}$ in the group of ChR-PsP & RN

Statistical analysis

In this study, we first used the Shapiro-Wilk test to assess the normality of the data. Data that followed a normal distribution were described using the mean ± standard deviation (Mean ± SD) and analyzed for group differences using the Independent Samples t-test. Data that did not follow a normal distribution were described using the median and interquartile range (Median [IQR]), with group differences evaluated using the Mann-Whitney U test. A receiver operating characteristic (ROC) curve analysis was conducted for each perfusion parameter. The area under the curve (AUC), sensitivity, and specificity were used to determine the optimal cutoff for differentiating iPsP from the ChR-PsP & RN. In all statistical analyses, a p-value of less than 0.05 was considered statistically significant. All statistical analyses were performed using IBM SPSS Statistics version 27.0 (IBM Corporation, Armonk, NY, USA).

Results

A total of 25 iPsP lesions in 16 patients and 48 ChR-PsP & RN lesions in 35 patients were enrolled in this study. All 16 iPsP patients had BMs from melanoma, lung cancer, and breast cancer. In the iPsP group, the mean age was 60.63 ± 10.84. Within the 35 patients with ChR-PsP & RN, 17 had malignant gliomas, and the other 18 patients had BMs. The mean age of these 35 patients in the ChR-PsP & RN group was 58.43 ± 11.63, Table 1. The median value of tumor sizes in the iPsP group was 1.43, which was potentially significantly lower than the ChR-PsP & RN group (2.64, $p=0.045$). There were no significant differences in tumor sizes between the iPsP group, the iPsP group and BM patients with ChR-PsP & RN (ChR-PsP & RN-BM), and the ChR-PsP & RN lesions in patients with malignant gliomas (ChR-PsP & RN-glioma).

The medians of $rCBV_{mean}$ and $rCBV_{max}$ values in iPsP and ChR-PsP & RN groups and the results of the Mann-Whitney U test were summarized in Table 1. The median values of $rCBV_{mean}$ and $rCBV_{max}$ in the group of iPsP were 0.94 and 1.39 respectively, which were significantly higher than the median values of $rCBV_{mean}$ and $rCBV_{max}$ in the group of ChR-PsP & RN (0.67, $p<0.01$, and 1.11, $p=0.01$, respectively), Fig. 2.

The comparison of the $rCBV_{mean}$ and $rCBV_{max}$ values between the iPsP group and BM patients with ChR-PsP & RN (ChR-PsP & RN-BM) showed significantly higher values of the iPsP group ($p=0.03$, and $p=0.01$, respectively). In contrast, compared to the ChR-PsP & RN-glioma group, the median $rCBV_{mean}$ values of the iPsP group were significantly increased (0.94 versus 0.48, $p<0.01$). The median $rCBV_{max}$ values of the iPsP group were higher than the $rCBV_{max}$ values of ChR-PsP & RN-glioma, but there was no

statistical significance (1.39 versus 1.11, $p=0.08$), Supplementary Fig. 1.

In addition, there was no statistical significance of the median $rCBV_{mean}$ and $rCBV_{max}$ values between sub-groups of ChR-PsP & RN-BM and ChR-PsP & RN-glioma ($rCBV_{mean}$ values of 0.73 and 0.48 respectively, $p=0.25$; $rCBV_{max}$ values of 1.05 and 1.11 respectively, $p=0.54$). The illustrative cases of iPsP and ChR-PsP & RN are in Figs. 3 and 4, both of which presented enlarged mass on the post-treatment conventional MRI.

The optimal cutoff of the $rCBV_{mean}$ value was 0.69, which can differentiate the iPsP from ChR-PsP & RN with an AUC of 0.71, sensitivity of 0.72, and specificity of 0.56. The optimal cutoff value of the $rCBV_{max}$ was 0.69 with an AUC of 0.683, sensitivity of 0.6, and specificity of 0.54.

Discussion

Our preliminary study showed that the $rCBV_{mean}$ and $rCBV_{max}$ values in the group of iPsP significantly increased compared to the group of ChR-PsP & RN. In the sub-group analysis, the iPsP $rCBV_{mean}$ value was significantly higher than the $rCBV_{mean}$ values of ChR-PsP & RN-BM and ChR-PsP & RN-glioma respectively. Compared to the ChR-PsP & RN-BM, the iPsP $rCBV_{max}$ value was significantly increased. The $rCBV_{max}$ value of iPsP was higher than the ChR-PsP & RN-glioma lesions, but the difference was not statistically significant. The optimal cutoff of the $rCBV_{mean}$ value was 0.69, which can differentiate the iPsP from ChR-PsP & RN with an AUC of 0.71, sensitivity of 0.72, and specificity of 0.56.

Similar to the high incidence of ChR-PsP, the overall incidence of iPsP ranges from 6% to 14.8% [20, 21], varying with the type of tumor treated with ICIs. One study noted iPsP in 17.9% of pembrolizumab treated patients [22].

In the present study, all 16 iPsP patients were treated with ICIs, which is consistent with the association of iPsP with the use of ICIs in previous studies [2, 3, 22].

There are three MR PWI techniques, including DSC, dynamic contrast-enhanced (DCE), and arterial spin labeling (ASL). Compared to DCE, MR DSC, and ASL are more commonly used in the neuro-oncology practice. ASL measures cerebral blood flow (CBF) noninvasively using magnetically labeled endogenous blood instead of contrast agents. MR DSC-PWI estimates the rCBV based on T2* signal intensity changes from the first passage of paramagnetic contrast agents through the cerebrovascular system.

There are few studies using DSC-PWI in the treatment response assessment of brain tumors following immunotherapy [23–28]. Their major findings are summarized in Table 2.

Cuccarini et al. [25] analyzed 18 TP and 8 iPsP lesions in 22 patients with newly diagnosed GBM treated with dendritic cell immunotherapy. They found that the difference of rCBV ($\triangle rCBV_{max}$) could effectively differentiate tumor recurrence from iPsP, with a sensitivity of 67% and specificity of 75% ($p=0.004$), suggesting that the rCBV modifications over time might be more helpful in distinguishing iPsP from TP. Vrabec et al. [24] reviewed 32 follow-up MRI examinations in 8 recurrent GBM patients treated with dendritic cell immunotherapy in a retrospective study; they found the highest $rCBV_{max}$ value (9.25 ± 2.68) was observed in the contrast-enhancing area of TP lesions, and the $rCBV_{max}$ value was higher even at time points before

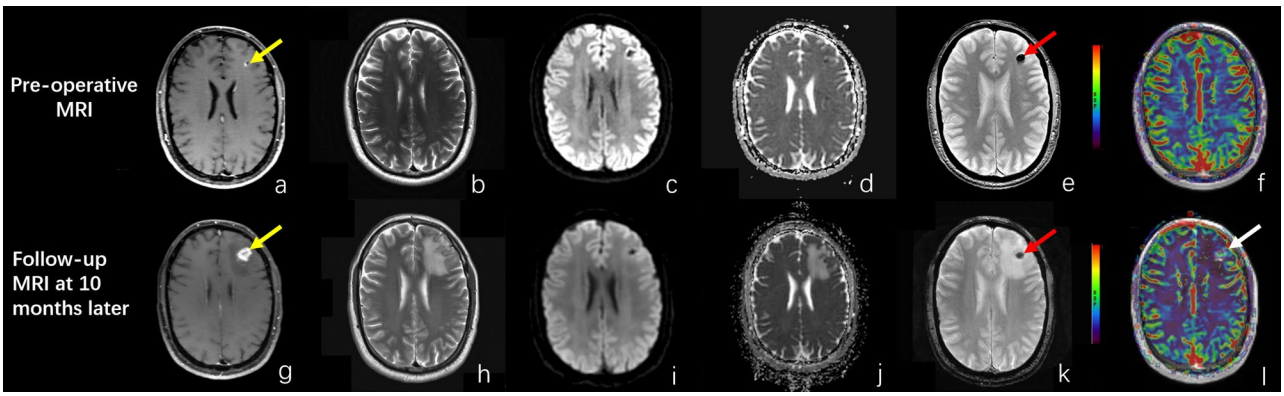

Fig. 3 An illustrative case of "iPsP" in BM. A patient with brain metastasis of melanoma was treated with Pembrolizumab and Ipilimumab. Figure **a** and Figure **g** are post-contrast 3D black blood Cube images. Figure **b** and Figure **h** are T2WI images. Figure **c** and Figure **i** are DWI images. Figure **d** and Figure **j** are ADC images. Figure **e** and Figure **k** are gradient recalled echo (GRE) images. Figure **f** and Figure **l** are CBV maps. MRI images in the first row are pre-immunotherapy treatment images. There was a small enhancing lesion (yellow arrow) in the left frontal lobe, with hypointensity (red arrow) on the GRE image. There was no elevated rCBV within this lesion. The MRI images of the second row are post-immunotherapy treatment images. There was a nodular enhancing mass (yellow arrow) in the left frontal lobe, with mildly increased rCBV (white arrow). This lesion was surgically removed, and "necrosis and treatment related changes" were diagnosed

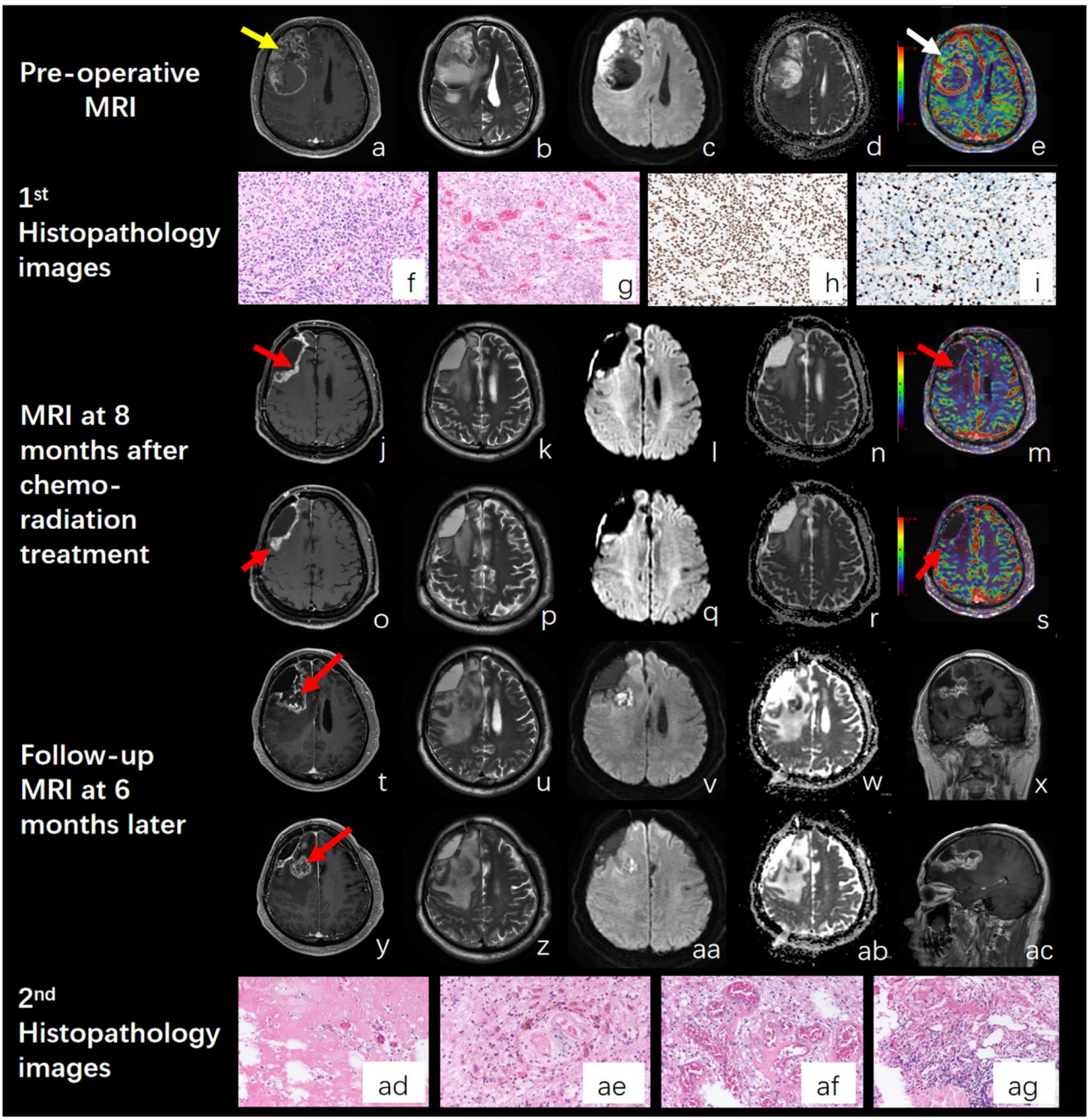

Fig. 4 An illustrative case of "ChR-PsP & RN". MRI images and histopathology images in a case of glioblastoma. Figures **a**, **j**, **o**, **t** and y are the post-contrast T1-BRAVO images. Figures **b**, **k**, **p**, **u**, and **z** are the T2WI images. Figures **c**, **i**, **q**, **v**, aa are the DWI images. Figures **d**, **n**, **r**, **w**, ab are the ADC map. Figures **e**, **m** and **s** are the CBV maps. Figure **x** and Figure ac are coronal and sagittal post-contrast T1-FLAIR images. Preoperative MRI images showed inhomogeneous nodular-ring enhancement (yellow arrow) with high rCBV (white arrow). After the first surgical resection, the histopathology images (Figure **f** and **g** of Hematoxylin-eosin staining, HE×100, h of the immunohistochemistry of ATRX (Alpha-thalassemia/mental retardation syndrome X-linked), and **i** of Ki-67). The lesion shows a high degree of cellular and nuclear polymorphism with numerous multinucleated giant cells. Microvascular proliferation is prominent. The expression of ATRX was strongly positive in tumor cells, and the Ki-67 index was about 50%. The follow-up MRI images after the standard chemo-radiation treatment showed nodular enhancements in the medial and poster walls of the surgical cavity, which raised the suspicion of TP. The CBV maps didn't demonstrate increased perfusion within the nodular enhancements (red arrow), suggesting the possibility of "pseudoprogression". Another MRI examination was performed 6 months later, revealing a large mass with heterogeneous peripheral enhancement resembling a "soap bubbles sign" (red arrow). The histopathology images of re-resected mass (HE, Figures ad-ag) showed extensive coagulative necrosis, the hyperplasia of glial cell, and accompanied by Fe-containing hemosiderin deposits, the vascular proliferation with vitelliform degeneration, and the foam cell and lymphocyte infiltration. The histopathology diagnosis was "necrosis and treatment related changes"

Table 2 Major MR DSC-PWI findings in the assessment of post-immunotherapy treatment response of brain tumors

Reference	Tumor type	Case number of pseudo-progression (treatment response)	Immunotherapy category	Evaluation parameters	Perfusion features (distinguishing pseudoprogression from true progression)
Song J, et al. [26]	Glioblastoma (recurrent)	7 cases / total 19 patients	immune checkpoint inhibitors (ICIs)	relative cerebral blood volume (rCBV)	Interval change in rCBV was not indicative of treatment response within 6 months after ICI treatment
Cuccarini V, et al. [25]	Glioblastoma (newly diagnosed)	8 pseudo-progression lesions / 22 patients	Dendritic Cell	relative cerebral blood volume (rCBV)	The difference of $\triangle rCBV_{max}$ could effectively differentiate tumor recurrence from pseudoprogression, with a sensitivity of 67% and specificity of 75%
Vrabec M, et al. [24]	Glioblastoma (recurrent)	5 patients (stable) /8 patients	Dendritic Cell	relative cerebral blood volume (rCBV)	Maximum lesional rCBV ratios were highest in group 1b (at or after progression) and were higher in group 1a (at time points before definite progression in progressive-tumour patients) compared to group 0 (stable during the follow-up period)
Stenberg L, et al. [23]	Glioblastoma	No information about pseudo-progression (treatment response) in six surgically and immunogene-treated patients	No detailed inforamtion of immunization therapy	relative cerebral blood volume (rCBV)	No differences of rCBV values were observed between the six immunized patients and the two non-immunized control patients.

definite progression (4.87 ± 1.61) compared to the $rCBV_{max}$ value of stable lesions (1.22 ± 0.47). They suggested that the $rCBV_{max}$ value was a potential radiological indicator to distinguish between immunotherapy-induced inflammatory response and recurrent GBM tumor growth. In a study that enrolled 79 examinations with DSC-PWI in 6 surgically/immunogene-treated GBM patients and two surgically treated GBM patients, Stenberg et al. showed that elevated rCBV, corresponding to the contrast-enhancing lesion, supports the diagnosis of recurrent GBM [23].

In a study conducted by Song et al. [26] 12 of the 19 recurrent GBM patients treated with ICIs were determined to have TP, and 7 had treatment responses after 6 months of ICI treatment (suggesting iPsP). They found that there was no significant difference in the absolute rCBV value and interval change in rCBV between the TP group and the treatment response group. The authors thought that the absolute rCBV value or interval change in rCBV was not indicative of treatment response within 6 months. A possible reason for the absence of significant difference in rCBV parameters between the TP group and the treatment response group may be associated with the confounding effects of anti-angiogenesis treatment [27]. In Song et al.'s study, there were 5 patients (26.3%) treated with bevacizumab before the commencement of ICIs and remained on this therapy throughout the entire period of study follow-up. Bevacizumab can alter perfusion characteristics by reducing angiogenesis, which may lead to perfusion changes without a statistically significant difference between TP and the treatment response groups.

Based on the literature review of Table 2, our study is the first study focusing on the comparison of perfusion features between the iPsP and ChR-PsP & RN in brain tumors. Our study is also the MR PWI study with the largest iPsP cohort.

Our study showed that there was no significant difference in the $rCBV_{mean}$ and $rCBV_{max}$ values between ChR-PsP & RN-BM and ChR-PsP & RN-glioma. The $rCBV_{mean}$ and $rCBV_{max}$ values of the iPsP group significantly increased compared to the group of ChR-PsP & RN. These findings supported the hypothesis that the mechanisms of iPsP and ChR-PsP & RN may be different. The mechanisms of ChR-PsP & RN have not yet been fully elucidated, they are speculated to be associated with the secondary reactions in the tumor area, including edema and abnormal vessel permeability, by the chemoradio-therapy induced tumour-cell and endothelial-cell killing, cell death, and the infiltration of inflammatory factors [2, 29, 30]. In contrast, the mechanisms of iPsP may be more complex, Dercle et al. thought they might be due to delayed activation of the immune system, local inflammation, and/or infiltration of tumor lesions and surrounding microenvironment by immune cells [2]. Our findings of significantly increased perfusion ($rCBV_{mean}$) of iPsP lesions than ChR-PsP & RN-BM and ChR-PsP & RN-glioma, indicated that this increased perfusion may be associated with local inflammation changes subsequent to restored antitumor immunity. Because of the distinct mechanisms of immunotherapy to activate the host immunity (beyond local infiltration of T-cells into the tumor environment) to treat cancers [3], the perfusion changes related to the restored antitumor capacity of the immune system are still unclear. In our study, the $rCBV_{max}$ values of ChR-PsP & RN-BM were lower than the $rCBV_{max}$ values of ChR-PsP & RN-glioma without statistically significant difference. These findings demonstrated the complexity

of immunotherapy-induced treatment changes. The difference of $rCBV_{max}$ values between iPsP and ChR-PsP & RN-glioma may suggest the variance of focal inflammations in the pseudoprogression lesions of malignant glioma patients. This difference may be affected by the limitation of our retrospective study in which the iPsP group only collected MR PWI data of BM patients treated with immunotherapy. In contrast, the published MR PWI studies of iPsP, summarized in Table 2, enrolled GBM patients. Future MR PWI studies with large cohorts including both BM and malignant glioma iPsP lesions may reveal more comprehensive perfusion features of such iPsP lesions [30].

We used the rCBV calculated with GE software as the hemodynamic biomarker of brain tumors in the present study. The rCBV was defined as CBV value of enhancing tumor divided by CBV value of reference white matter. Compared to other quantitative parameters which are measured within the enhancing tumors, the application of the semi-quantitative parameter of rCBV may result in less variations among different MR scanners. Previous studies showed that the rCBV results had significant difference between 1.5T and 3T, and differed from different software packages [31, 32]. In addition, the accurate rCBV measurement may be affected by the combination treatment of immunotherapy and anti-angiogenesis therapy [30].

This study has several limitations. Firstly, the sample size of the present study was relatively small. Secondly, our study focused on the MR perfusion changes of the iPsP lesions, however, there was no glioma patient with iPsP lesion having valid MR perfusion data in this retrospective study, thus the enrollment of iPsP lesions may have an inclusion bias. Thirdly, in this study, we found significant perfusion changes of $rCBV_{mean}$ and $rCBV_{max}$, in addition, we also noticed interesting biostatistics findings of tumor size in the iPsP lesions. Future studies with deeper perfusion features, such as histogram analysis or radiomics analysis, combined with more MR structural imaging parameters may be more useful in detecting inherent abnormalities of iPsP than the ROIs-based perfusion measurements. Finally, the present study analyzed iPsP lesions of BMs, which often had an intra-tumoral hemorrhage, which has been shown to limit the perfusion measurement of DSC-PWI [6–14].

Conclusion

In this preliminary study, we found that the $rCBV_{mean}$ and $rCBV_{max}$ values of the iPsP group were significantly higher than ChR-PsP & RN group. These findings may suggest immunotherapy-induced significantly increased perfusion changes of iPsP lesions than the ChR-PsP & RN lesions in primary and metastatic brain tumors.

Supplementary Information The online version contains supplementary material available at https://doi.org/10.1007/s11060-024-04910-0.

Author contributions HZW and XL were involved in conception and design of the research. CH, QL and YcH contributed to acquisition of data. GT, WH, and DS were involved in analysis and interpretation of the data. CH, GT, LZ and HJ contributed to statistical analysis. CH, XL, YH and GT were involved in writing of the manuscript. HZW, RB, YH and SMS contributed to critical revision of the manuscript for intellectual content. all authors commented on previous versions of the manuscript. All authors read and approved the final manuscript.

Funding This work was supported by Scientists in the Bureau of Science and Technology of ShaoGuan (Grant No. 230329238033088, No. 230330208036590, No. 220531214533619), the National Natural Science Foundation of China (No. 82202983), and the Peking University Clinical Scientist Training Program, funded by the Fundamental Research Funds for the Central Universities. Author XL has received research support from Scientists in the Bureau of Science and Technology of ShaoGuan. Author HJ has received research support from the National Natural Science Foundation of China and the Fundamental Research Funds for the Central Universities.

Data availability No datasets were generated or analyzed during the current study.

Declarations

Ethical approval This retrospective study was approved by the ethics committees of the Yuebei People's Hospital, and the requirement for informed consent was waived (Date August 1, 2022 /No. KY-2022-042).

Consent to participate The requirement for informed consent was waived.

Competing interests The authors declare no competing interests.

References

1. Wen PY, van den Bent M, Youssef G et al (2023) RANO 2.0: update to the Response Assessment in Neuro-Oncology Criteria for High- and low-Grade gliomas in adults. J Clin Oncol 41:5187–5199

2. Dercle L, Sun S, Seban RD et al (2023) Emerging and evolving concepts in Cancer Immunotherapy Imaging. Radiology 306:e239003
3. Nishino M, Hatabu H, Hodi FS (2019) Imaging of Cancer Immunotherapy: current approaches and future directions. Radiology 290:9–22
4. Ellingson BM, Wen PY, Cloughesy TF (2017) Modified Criteria for Radiographic Response Assessment in Glioblastoma clinical trials. Neurotherapeutics 14:307–320
5. Lin NU, Lee EQ, Aoyama H et al (2015) Response assessment criteria for brain metastases: proposal from the RANO group. Lancet Oncol 16:e270–278
6. Wang S, Martinez-Lage M, Sakai Y et al (2016) Differentiating Tumor Progression from Pseudoprogression in patients with Glioblastomas using Diffusion Tensor Imaging and Dynamic susceptibility contrast MRI. AJNR Am J Neuroradiol 37:28–36
7. Roques M, Catalaa I, Raveneau M et al (2022) Assessment of the hypervascularized fraction of glioblastomas using a volume analysis of dynamic susceptibility contrast-enhanced MRI may help to identify pseudoprogression. PLoS ONE 17:e0270216
8. Anil A, Stokes AM, Chao R et al (2023) Identification of single-dose, dual-echo based CBV threshold for fractional tumor burden mapping in recurrent glioblastoma. Front Oncol 13:1046629
9. Nierobisch N, Ludovichetti R, Kadali K et al (2023) Comparison of clinically available dynamic susceptibility contrast post processing software to differentiate progression from pseudoprogression in post-treatment high grade glioma. Eur J Radiol 167:111076
10. Barajas RF, Chang JS, Sneed PK, Segal MR, McDermott MW, Cha S (2009) Distinguishing recurrent intra-axial metastatic tumor from radiation necrosis following gamma knife radiosurgery using dynamic susceptibility-weighted contrast-enhanced perfusion MR imaging. AJNR Am J Neuroradiol 30:367–372
11. Mitsuya K, Nakasu Y, Horiguchi S et al (2010) Perfusion weighted magnetic resonance imaging to distinguish the recurrence of metastatic brain tumors from radiation necrosis after stereotactic radiosurgery. J Neurooncol 99:81–88
12. Huang J, Wang AM, Shetty A et al (2011) Differentiation between intra-axial metastatic tumor progression and radiation injury following fractionated radiation therapy or stereotactic radiosurgery using MR spectroscopy, perfusion MR imaging or volume progression modeling. Magn Reson Imaging 29:993–1001
13. Wang B, Zhao B, Zhang Y et al (2018) Absolute CBV for the differentiation of recurrence and radionecrosis of brain metastases after gamma knife radiotherapy: a comparison with relative CBV. Clin Radiol 73:758 e751-758 e757
14. Morabito R, Alafaci C, Pergolizzi S et al (2019) DCE and DSC perfusion MRI diagnostic accuracy in the follow-up of primary and metastatic intra-axial brain tumors treated by radiosurgery with cyberknife. Radiat Oncol 14:65
15. Korman AJ, Garrett-Thomson SC, Lonberg N (2022) The foundations of immune checkpoint blockade and the ipilimumab approval decennial. Nat Rev Drug Discov 21:509–528
16. Smith DA, Kikano E, Tirumani SH, de Lima M, Caimi P, Ramaiya NH (2022) Imaging-based Toxicity and Response Pattern Assessment following CAR T-Cell therapy. Radiology 302:438–445
17. Marei HE, Hasan A, Pozzoli G, Cenciarelli C (2023) Cancer immunotherapy with immune checkpoint inhibitors (ICIs): potential, mechanisms of resistance, and strategies for reinvigorating T cell responsiveness when resistance is acquired. Cancer Cell Int 23:64
18. Alimonti P, Gonzalez Castro LN (2023) The current Landscape of Immune checkpoint inhibitor immunotherapy for primary and metastatic brain tumors. Antibodies (Basel) 12(2):27. https://doi.org/10.3390/antib12020027
19. Okada H, Weller M, Huang R et al (2015) Immunotherapy response assessment in neuro-oncology: a report of the RANO working group. Lancet Oncol 16:e534–e542
20. Frelaut M, du Rusquec P, de Moura A, Le Tourneau C, Borcoman E (2020) Pseudoprogression and Hyperprogression as New forms of response to Immunotherapy. BioDrugs 34:463–476
21. Kim N, Lee ES, Won SE et al (2022) Evolution of Radiological Treatment Response assessments for Cancer Immunotherapy: from iRECIST to Radiomics and Artificial Intelligence. Korean J Radiol 23:1089–1101
22. Ahmed FS, Dercle L, Goldmacher GV et al (2021) Comparing RECIST 1.1 and iRECIST in advanced melanoma patients treated with pembrolizumab in a phase II clinical trial. Eur Radiol 31:1853–1862
23. Stenberg L, Englund E, Wirestam R, Siesjö P, Salford LG, Larsson EM (2006) Dynamic susceptibility contrast-enhanced perfusion magnetic resonance (MR) imaging combined with contrast-enhanced MR imaging in the follow-up of immunogene-treated glioblastoma multiforme. Acta Radiol 47:852–861
24. Vrabec M, Van Cauter S, Himmelreich U et al (2011) MR perfusion and diffusion imaging in the follow-up of recurrent glioblastoma treated with dendritic cell immunotherapy: a pilot study. Neuroradiology 53:721–731
25. Cuccarini V, Aquino D, Gioppo A et al (2019) Advanced MRI Assessment during dendritic cell Immunotherapy added to Standard Treatment against Glioblastoma. J Clin Med 8
26. Song J, Kadaba P, Kravitz A et al (2020) Multiparametric MRI for early identification of therapeutic response in recurrent glioblastoma treated with immune checkpoint inhibitors. Neuro Oncol 22:1658–1666
27. Chawla S, Shehu V, Gupta PK, Nath K, Poptani H (2021) Physiological imaging methods for evaluating response to immunotherapies in Glioblastomas. Int J Mol Sci 22
28. Lee J, Chen MM, Liu HL, Ucisik FE, Wintermark M, Kumar VA (2024) MR Perfusion Imaging for Gliomas. Magn Reson Imaging Clin N Am 32:73–83
29. Brandsma D, Stalpers L, Taal W, Sminia P, van den Bent MJ (2008) Clinical features, mechanisms, and management of pseudoprogression in malignant gliomas. Lancet Oncol 9:453–461
30. Liu X, Chen H, Tan G et al (2024) A comprehensive neuroimaging review of the primary and metastatic brain tumors treated with immunotherapy: current status, and the application of advanced imaging approaches and artificial intelligence. Frontiers in Immunology. https://doi.org/10.3389/fimmu.2024.1496627
31. Kudo K, Uwano I, Hirai T et al (2017) Comparison of different post-processing algorithms for dynamic susceptibility contrast Perfusion Imaging of cerebral gliomas. Magn Reson Med Sci 16:129–136
32. Mauz N, Krainik A, Tropres I et al (2012) Perfusion magnetic resonance imaging: comparison of semiologic characteristics in first-pass perfusion of brain tumors at 1.5 and 3 Tesla. J Neuroradiol 39:308–316